

Optometric Methods for Testing Sections of Buckling

Abstract: The article presents a study aimed to experimentally identify the correlation between the deflection arrow of a buckled flat bar and the magnitude of applied force P as well as to determine the value of critical force necessary for maintaining the equilibrium of the flat bar in its bent form. The study-related tests involved the use of a Gleeble 3800 metallurgical process simulator. Based on the data obtained in the tests and using Euler's equation, it was possible to determine the transverse modulus of elasticity. An inductance-type extensometer (usually used in the Gleeble simulator) and a digital image correlation system (used in both the visible and ultraviolet light configuration) were applied to record changes in the length of the flat bar in time. The study also included the investigation of methods used when marking the surface of materials subjected to measurements involving the use of digital image correlation, i.e.:

- covering the surface with light-coloured paint and depositing the “speckled pattern”,
- deposition of the “speckled pattern” in the form of an impression using a microhardness tester,
- deposition of the “speckled pattern” in the form of a pattern burnt out by the laser beam on the specimen surface.

Key words: stability of sections, Digital Image Correlation, Young's modulus, stable equilibrium, unstable equilibrium, elastic buckling, Euler critical force

1. Introduction

1.1. Types of equilibrium

According to S.P. Timoshenko [1], there are several types of body equilibrium (Fig.1), i.e.:

- stable equilibrium – form of equilibrium, in which a body swung out of its original position spontaneously returns to the latter. For the body located in the potential field of forces, the position of stable equilibrium corresponds to the minimum of potential energy.
- unstable equilibrium – form of equilibrium, in which a body swung out of its original position moves to another position. For the body located in the potential field of forces, the position of stable equilibrium corresponds to the maximum of potential energy.
- neutral equilibrium – represents a special type of equilibrium, in which, at any small tilt, the value of potential energy remains unchanged.

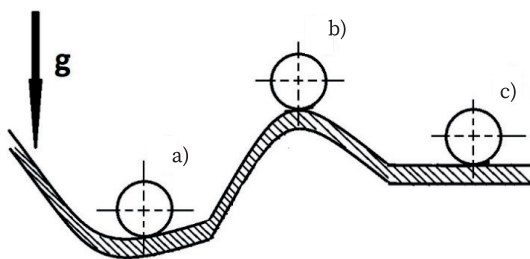


Fig. 1. Types of body equilibrium: a) stable, b) unstable and c) neutral

Bodies in unstable equilibrium seek to pass from one position to another. Such a transition is characterised by large displacements, the generation of plastic strains or even irreparable damage to the system [2]. The aforesaid form of transition from one position to another is referred to as the loss of stability. If bringing the system into unstable equilibrium can be triggered by such a small amount of energy that it can be provided by chance, the stability of the system is insufficient.

In addition to the geometrical form, stability also depends on the magnitude of (acting) forces. In many existing structures, elements decisive for stability are axially compressed bars, making the issue of buckling an important part of engineering calculations. The loss of stability does not always lead to the failure of an element but always results in the loss of structural load-carrying capacity. The risk of stability loss decreases along with an increase in the weight of the structure [3]. The aforesaid issue is important as the loss of stability takes place suddenly, without any “warning” symptoms preceding the unsafe condition of the structure.

1.2. Loss of stability of compressed bars

In contrast to rigid deformable systems, values of existing forces significantly affect the type of equilibrium. Static force Q , perpendicular to the axis of the bar compressed by force P along the axis leads to the deflection of the bar. Once force Q has been withdrawn, the bar returns to its original form. If the action of force Q is dynamic, it triggers the vibration of the bar around the axis. An increase in the value of force P initially increases the period of

vibration but, after exceeding the characteristic and critical value (critical force P_{kr}) and after the momentary action of force Q , the bar does not return to its original form, but finds itself in a new state, i.e. stable (constant) equilibrium of deflected axis (connected with an abrupt increase in bar tip displacements). The above-presented phenomenon is referred to as buckling [3].

1.3. Elastic buckling of the bar

The elastic buckling of the bar is the case of stability loss, where the critical force triggers the generation of normal stresses lower than proportional limit R_h [8]. The Euler equation, determining the value of critical force P_{cr} , was derived assuming that the bar was compressed axially and supported bilaterally and pinned (Fig. 2). If support conditions do not determine the direction of bar deflection, the latter takes place in the plane of the least bending rigidity $EI = EI_{min}$. In the state of equilibrium in the bent form, there is an additional bending moment, the value of which in the section is the following [10]:

$$M_g = P_y \tag{1}$$

The equation of the deflected axis has the following form:

$$EI_g \frac{d^2y}{dx^2} = -M_g \tag{2}$$

which can be expressed as follows:

$$EI \frac{d^2y}{dx^2} = -Py \tag{3}$$

The transformation of dependence (3) leads to the obtainment of the following equation:

$$\frac{d^2y}{dx^2} + \frac{Py}{EI} = 0 \tag{4}$$

The above-presented equation can be used to determine force. After appropriate transformations [2], it is possible to calculate the so-called Eulerian critical force, i.e. the maximum compressive force, for which it is possible to maintain the equilibrium of the bar in the bent form [9].

$$P_{kr} = \frac{\pi^2 EI}{l^2} \tag{5}$$

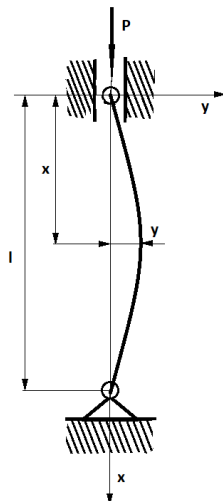


Fig. 2. Axially compressed straight bar

General cases require providing the following dependence, taking into count various modes of support:

$$P_{kr} = \frac{\pi^2 EI}{l_w^2} \tag{6}$$

where:

$l_w = \mu l$ – buckling length of the bar,

μ – coefficient dependent on the bar fixing method (Tab. 1).

The determination of critical stress requires the division of critical force by bar cross-sectional area A :

$$\sigma_{kr} = \frac{\pi^2 EI_{min}}{A l_w^2} = \frac{\pi^2 E i_{min}^2}{l_w^2} \tag{7}$$

where:

$i = \sqrt{\frac{I}{A}}$ – radius of the inertia of the bar cross-section.

From equation (7) it is possible to extract a parameter referred to as the slenderness of the flat bar (8)

$$\lambda = \frac{l_w}{i} \tag{8}$$

Formula (7) can be expressed in the graphic form, i.e. as the Eulerian hyperbola (Fig. 3). The Euler equation is only applicable within the elastic range ($\sigma_{kr} < \sigma_H$).

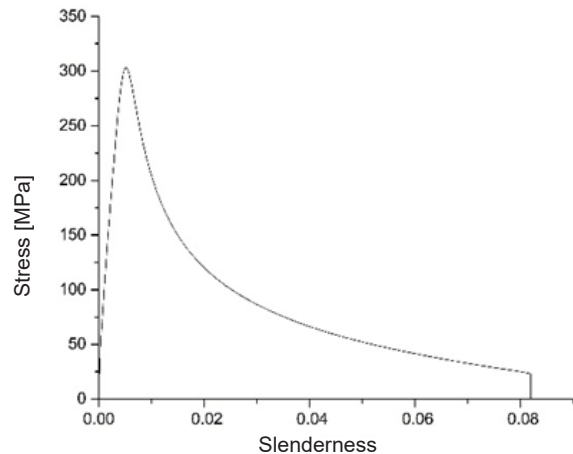


Fig. 3. Dependence of critical stresses on the slenderness of the buckling bar

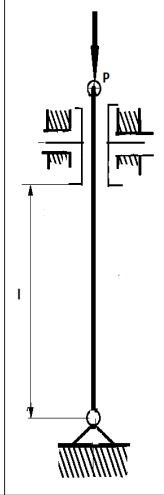
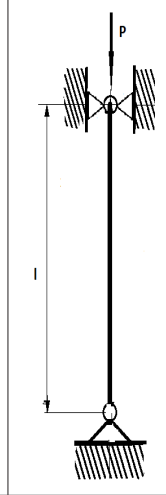
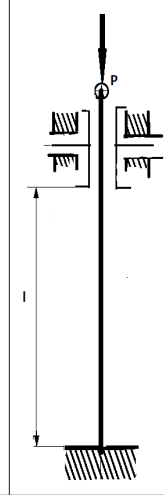
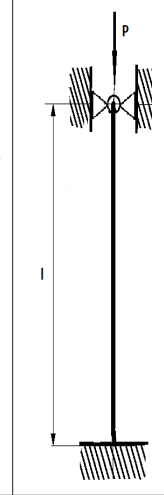
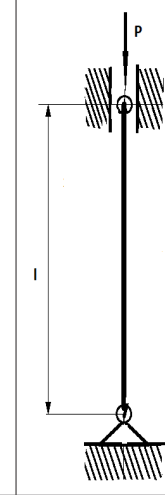
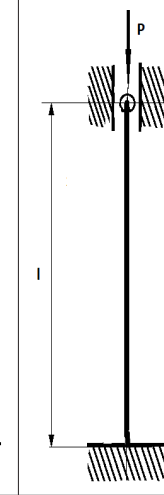
The limiting slenderness ratio is determined using the following dependence:

$$\lambda_{gr} = \sqrt{\frac{E}{\sigma_H}} \tag{9}$$

2. Research objective

The objective of the study discussed in the article was to identify buckling properties of a flat bar made of dual-phase steel AISI 316L as well as to propose a digital image correlation method as the method enabling measurements of length changes in such tests. The study also involved the testing of a method used for the marking of specimens by means of a laser welding machine and a microhardness tester (in order to create the so-called “speckles” on the surface of test specimens using digital image correlation).

Table 1. Coefficients for various bar fixing methods

Schematic diagram							
μ	2	2	1	1	0.699	0.699	0.5

3. Testing methodology

3.1. Test material

The tests involved the use of flat bars made of steel AISI 316L, having the geometry as presented in Figure 4 and the mass fraction of elements presented in w Table 2.

Table 2. Percentage fraction of chemical elements in the test material

Element	Fe	Mn	Ni	Cr
Fraction [%]	97.95	1.45	0.31	0.29

3.2. Test rig

3.2.1. Gleeble 3800 simulator of metallurgical processes

The device imposing a load affecting the specimen was a Gleeble 3800 simulator in the “Pocket Jaw” configuration. The technical parameters of the machine made it possible to simulate various types of experiments and technological processes.

3.2.2. Inductance-type extensometer

One of the more important parameters investigated within the tests was a change in the length of the specimen in time (measured using three sensors). The first of the measurement devices was an “L Gauge” inductance-type extensometer (Fig. 5).

The above-named extensometer was resistant to high temperature and characterised by theoretically infinite resolution. The device only recorded changes in the direction of measurement, yet, in addition to the specimen, its range also included the grips of the loading device (which increased measurement uncertainty).

3.2.3. Digital Image Correlation System

When testing structural elements for buckling, an important parameter subjected to measurements is the change of the specimen length. The maintaining of high measurement precision requires the placement of the gauge directly on the test specimen. However, the specific movement of the specimen undergoing deformation may destroy the extensometer whiskers nearing the material surface or trigger the loss of contact between the whiskers and the material (thus

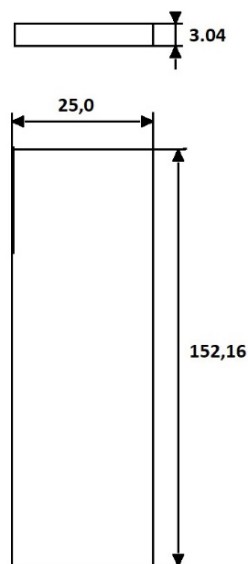


Fig. 4. Geometry of test specimens

precluding the recording of data). A solution to this problem could involve the use of non-contact deformation measurement methods, e.g. digital image correlation.

Digital image correlation is used in measurements of deformations based on the recording and comparison of a

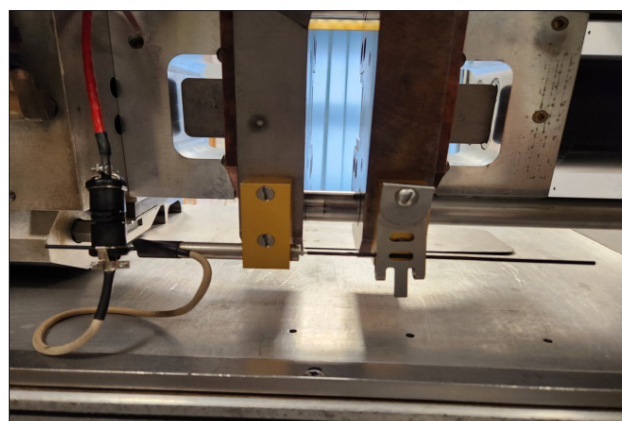


Fig. 5. Inductance-type extensometer

series of digital images. The performance of measurements must be preceded by marking the test surface with a speckled pattern [6]. Depending on its version, the device consists of one (2D) or two (3D) cameras and a light source. The tests involved the use of two 2D systems. One included a high-speed camera operating in visible light, whereas the other one (proposed by the Author) was composed of an ultraviolet light source having a power of 100W and a wavelength of 365 nm as well as a recorder, i.e. a D3100 camera (Nikon) (appropriately modified to enable the recording of images in UV light) (Fig. 6).

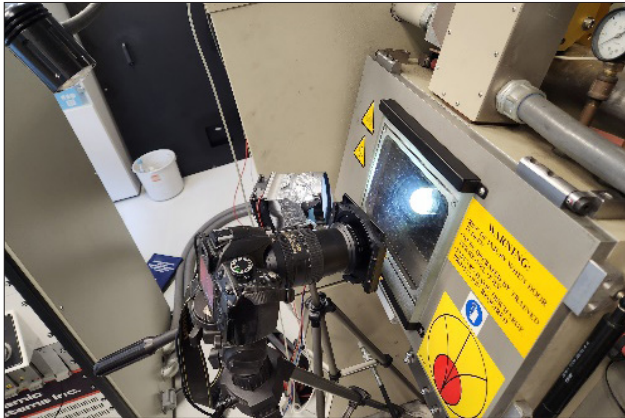


Fig. 6. Ultraviolet digital image correlation system

3.3. Experiment

The tests specimens were 3 flat bars made of steel AISI 316L (Fig. 4). Each specimen was provided with the speckled pattern, applied using different techniques:

- specimen no.1 was covered with white Nulifire paint and black “speckles” (applied on the white paint-coated surface using “VHT Flame Proof” spray paint),
- specimen no. 2 was covered with the speckled patterns using the low-power laser beam,
- pattern on specimen no. 3 was created using a microhardness tester.

Figure 7 presents the surfaces of the test specimens.

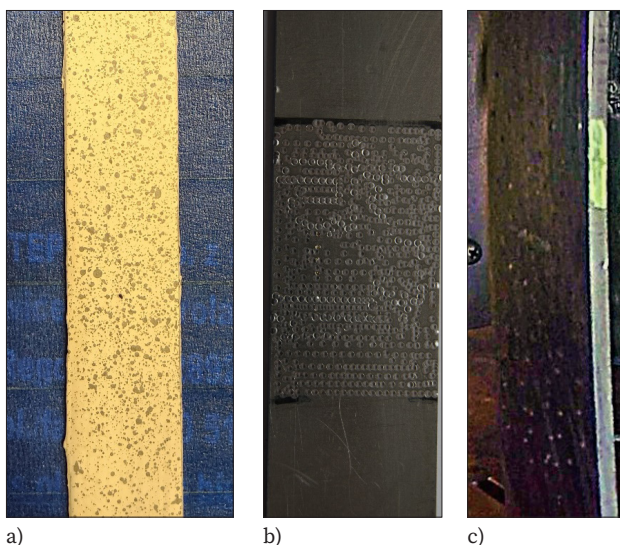


Fig. 7. Specimen markers: a) paints, b) laser beam and c) microhardness tester

Each specimen was subjected to axial compression exerted at a tool movement rate of 0.1mm/s and a temperature of 20 °C. The experiment was continued until the exceeding of the yield point of the material [4]. The deformation of each specimen was recorded using the aforementioned DIC system provided with a high-speed camera, the UV-DIC system and the inductance-type extensometer. Data recorded in the tests were used to determine the Euler hyperbola, the correlation between the arrow of deflection and the change of flat bar length $y_1 = f(y_1/P)$ as well as to identify the value of critical force and the material-related Young's modulus (for each set of data).

4. Test results

Deformations of each specimen were recorded by 3 independent measurement systems. The performance of measurements enabled the comparison of the methods used for the marking of specimen surfaces.

4.1. Laser-marked specimen

Unlike in classical, i.e. dye-based marking systems, the pattern was created using the point-like heat treatment of the material. Such an approach eliminated the risk of speckle cracking and the degradation of the pattern on the specimen. However, the method involved the point-like and high temperature-triggered changes in the material structure. In order to reduce the above-presented adverse effect of temperature on experimentation results, only the thin subsurface layer of the material could be exposed to the effect of laser beam. Regrettably, the aforesaid restriction resulted in the poor quality of the pattern, which ultimately precluded the recording of deformations, both in visible and ultraviolet light (Fig. 8).

4.2. Specimen marked using the microhardness tester

Unlike in classical, i.e. dye-based marking systems, the pattern was created by impressing dots (speckles) on the material surface. Such an approach eliminated the risk of speckle cracking and the degradation of the pattern on the specimen. However, the method was connected with the point-like deformation of the material. In addition, the contrast between the speckles and the background was low and varied depending on the light beam angle of incidence. The deformation of the material was also responsible for changes of the points making up the speckled pattern. As a result, the quality of the pattern was overly low to be recordable in visible light (Fig. 9). The UV-DIC enabled the recording of only a small part of the curve.

4.3. Dye-marked specimen

The classic method used for the marking of the specimen surface resulted in the formation of a good-quality pattern and enabled the recording of deformations throughout the experiment, both in ultraviolet and visible light (Fig. 10).

4.4. Euler's hyperbola

The data recorded by the inductance-type sensor (in relation to each specimen), the data obtained using digital image correlation (both in visible and ultraviolet light) in relation to the paint-coated specimen as well as the data

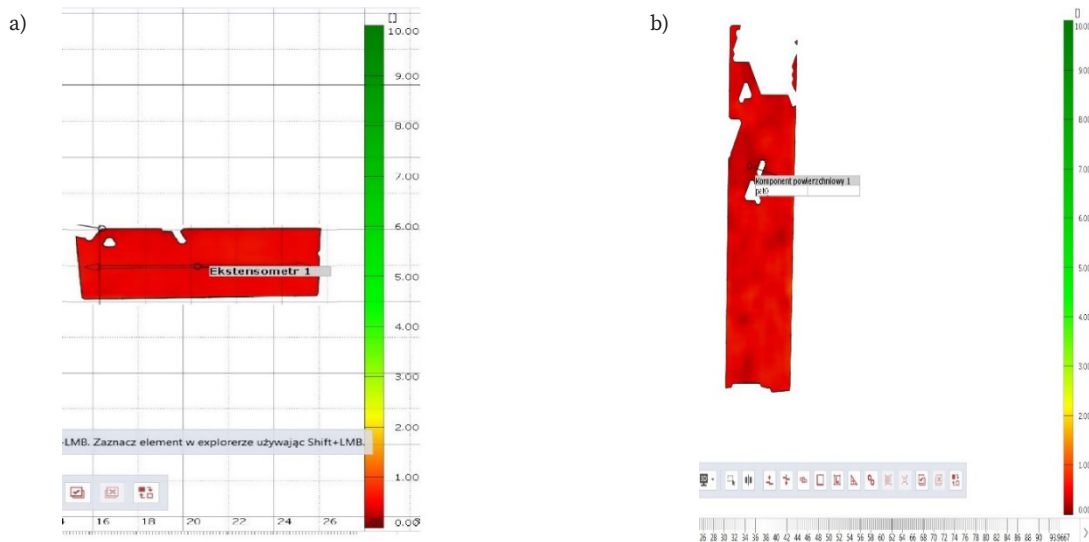


Fig. 8. Quality of the pattern burnt out using the laser beam: a) in visible light and b) in ultraviolet light



Fig. 9. Quality of the pattern obtained using the microhardness tester (in visible light)

obtained using UV-DIC and concerning the specimen marked by means of the microhardness tester were used to identify the dependence of critical stress (7) on the slenderness of the flat bar (8). The adopted bar fixing coefficient amounted to 0.5, whereas the radius of the inertia of the cross-section of the flat bar amounted to 0.88mm. The curves identified in the test are presented in Fig. 11.

4.5. Correlation between the arrow of deflection and the change in the flat bar length

The correlation between the arrow of deflection and the change in the flat bar length (in relation to each data set) was as follows (Fig. 12).

4.6. Critical force

The data concerning the correlation between the arrow of deflection [5] and the change in the flat bar length were used to determine critical force for each case under investigation. The results are presented in Table 3.

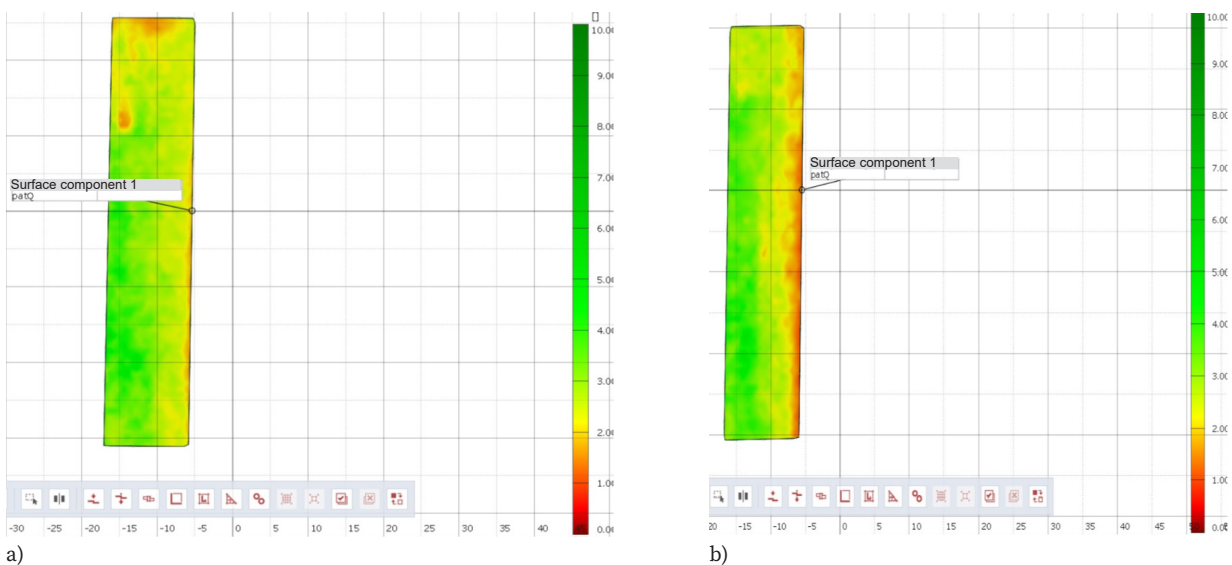


Fig. 10. Quality of the pattern obtained using paints: a) in visible light and b) in ultraviolet light

Table 3. Critical force values obtained in the cases subjected to analysis

Test	Paint-coated specimen, recorded using the extensometer	Paint-coated specimen, recorded using DIC in visible light	Paint-coated specimen, recorded using UV-DIC	Specimen marked using the laser beam, recorded using the extensometer	Specimen marked using the microhardness tester, recorded using the extensometer
P_{kr} [kN]	256.55	214.76	215.12	256.49	218.83

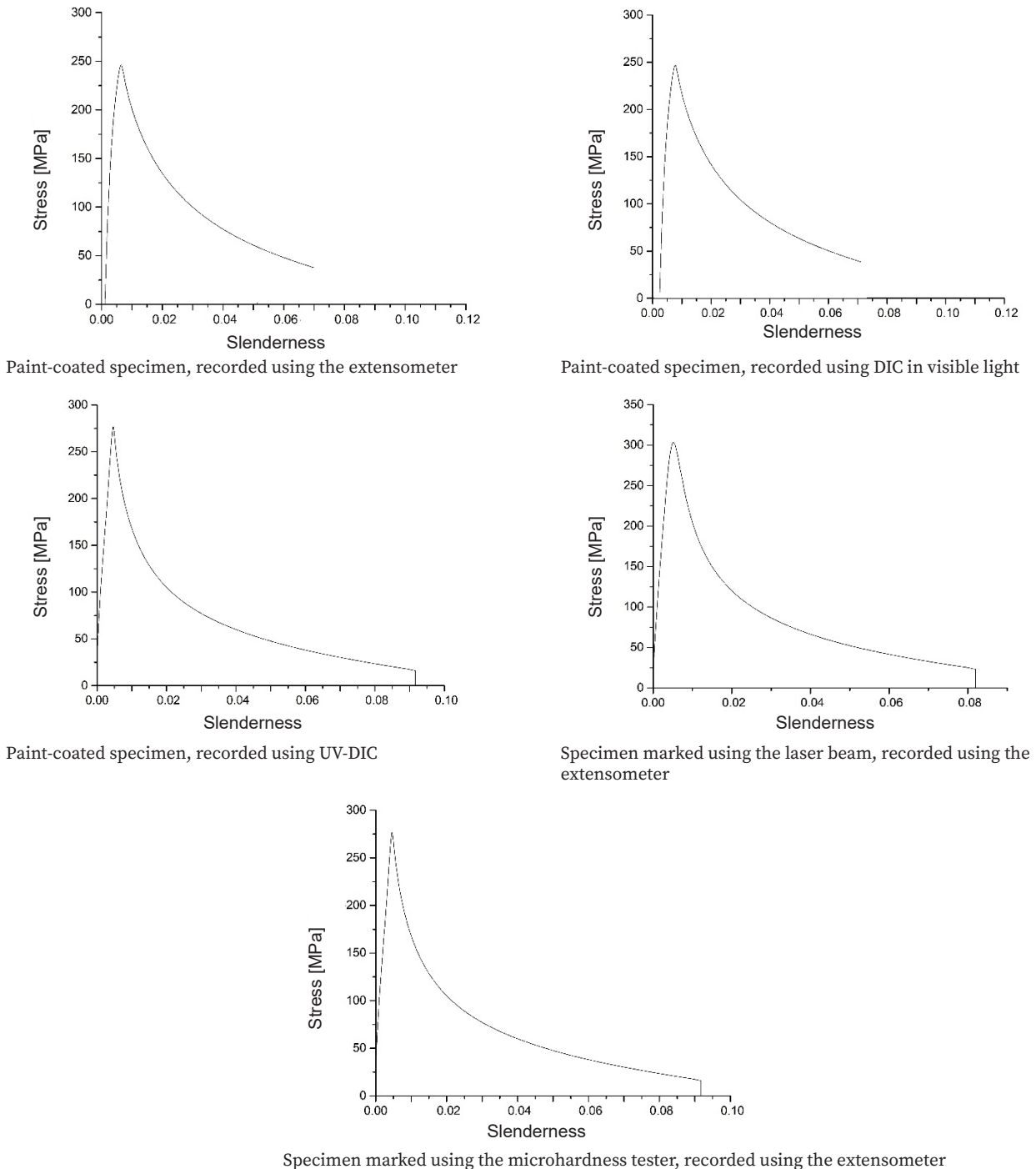


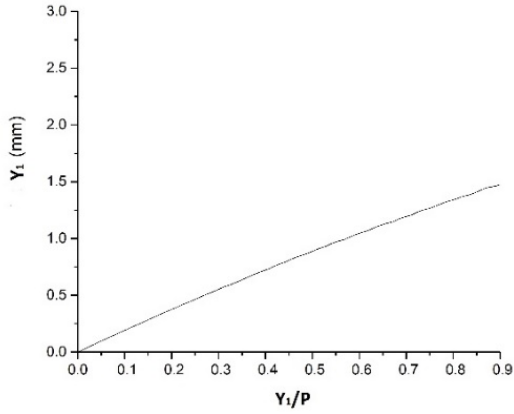
Fig. 11. Euler's hyperbola in relation to measurement results subjected to analysis

4.7. Young's modulus

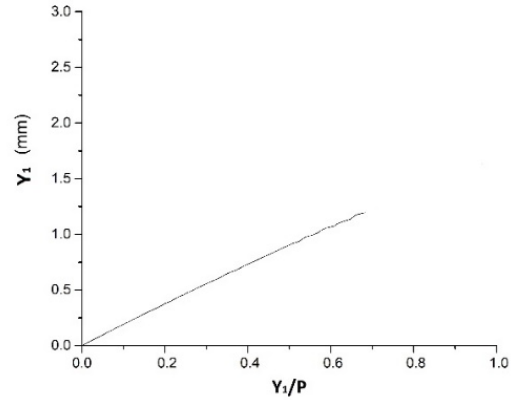
The transformation of dependence (6) enabled the determination of Young's modulus in relation to each set of data (tab. 4).

5. Discussion

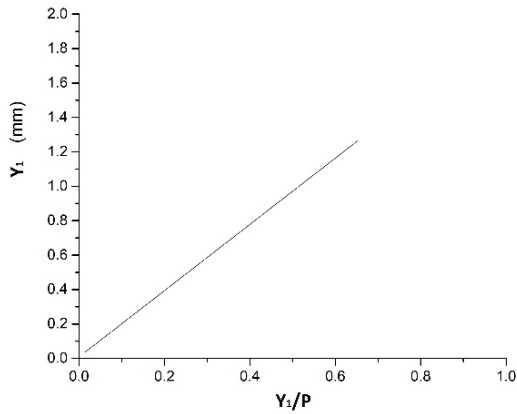
All the test results exceeded the value of critical force (see Fig. 13). The results of the buckling tests involving the flat bars made of steel AISI316L revealed discrepancy,



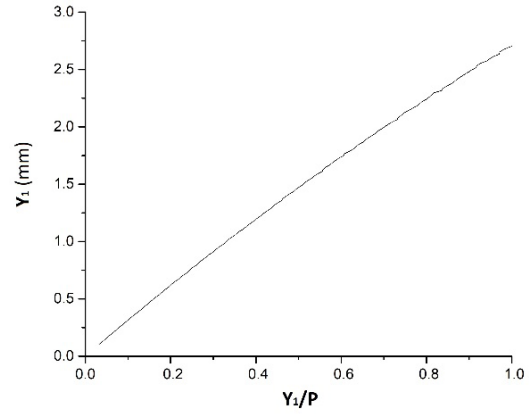
Paint-coated specimen, recorded using the extensometer



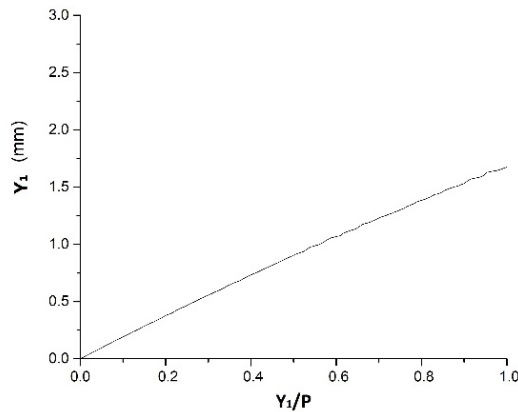
Paint-coated specimen, recorded using DIC in visible light



Paint-coated specimen, recorded using UV-DIC



Specimen marked using the laser beam, recorded using the extensometer



Specimen marked using the microhardness tester, recorded using the extensometer

Fig. 12. Correlation between the arrow of deflection and the change in the flat bar length

Table 4. Critical force values obtained in the cases subjected to analysis

Test	Paint-coated specimen, recorded using the extensometer	Paint-coated specimen, recorded using DIC in visible light	Paint-coated specimen, recorded using UV-DIC	Specimen marked using the laser beam, recorded using the extensometer	Specimen marked using the microhardness tester, recorded using the extensometer
E[GPa]	256.56	201.96	200.89	268.40	295.30

yet the values concerning Young’s modulus [10] were consistent with information found in reference publications. The aforementioned discrepancy in the results could be ascribed to the following factors:

- range of the inductance-type extensometer included not only the specimen but also the grips of the device, which translated into increased measurement uncertainty,



Fig. 13. Specimens after the tests: a) no. 1, b) no. 2 and c) no. 3

- result-related differences could also be attributed to the application of various methods used when recording material deformations,
- manner, in which the specimens were cut out of the sheet, i.e. the specimen marked using paint and that marked by means of the laser beam were cut out along the direction of rolling, whereas the specimen marked using the microhardness tester was cut out perpendicularly to the direction of rolling. The anisotropy of grains in the material directly affected the properties of the specimens.

6. Wnioski

Concluding remarks:

- methods used for the marking of the test specimens (using digital image correlation) failed to meet previously assumed requirements,
- pattern created using the laser beam proved insufficient as regards the recording of deformations, both in visible and ultraviolet light,
- pattern obtained by means of the microhardness tester also proved insufficient for the recording of deformations in visible light. Some data were successfully recorded in ultraviolet light, yet their amount was insufficient in terms of further analyses. In addition, it was possible to observe the deformation of speckles created on the material surface, which definitely “disqualified” the above-named marking method,
- classical method involving the deposition of speckles using two contrasting paints enabled the recording of deformations throughout the experiment in both types of light (visible and UV). The differences between the data recorded using digital image correlation and the data obtained using the inductance-type extensometer resulted from various values of measurement uncertainties of both devices.

The DIC system can be used for the recording of deformations in buckling tests, yet the methods discussed in the article failed to fulfil their role. The measurement results obtained using the system differed from those obtained using the inductance-type extensometer. The comparability of results obtained in the future by means of both devices will require necessary corrections.

The Author intends to continue research concerning the issue discussed in the article, particularly as regards the behaviour of specimens in buckling tests performed at higher temperature.

LITERATURA

- [1] Timoshenko S.P.: Teoria stateczności prętów. Arkady, Warszawa, 1961.
- [2] Dyląg Z., Jakubowicz A., Orłoś Z.: Wytrzymałość materiałów, t. I-II. Wydawnictwa Naukowo-Techniczne, Warszawa 1996-97.
- [3] Bąk R., Burczyński T.: Wytrzymałość materiałów z elementami ujęcia komputerowego. Wydawnictwa Naukowo-Techniczne, Warszawa 2001.
- [4] Bieluch W., Burczyński T., Fedeliński P., John A., Kokot G., Kuś W.: Laboratorium z wytrzymałości materiałów. Wydawnictwo Politechniki Śląskiej, skrypt nr 2285, Gliwice 2002.
- [5] Zienkiewicz O.C.: Metoda elementów skończonych. Arkady, Warszawa 1972.
- [6] Marcinczak D.: Wzmacnianie konstrukcji betonowych za pomocą materiałów kompozytowych. Nauka i Budownictwo, 2019, no. 66.
- [7] Niezgodziński M.E., Niezgodziński T.: Wzory, wykresy i tablice wytrzymałościowe. PWN, Warszawa 1973.
- [8] Katarzyński S., Końcada S., Zakrzewski M.: Badania własności mechanicznych metali. Wydawnictwa Naukowo-Techniczne, Warszawa 1969.
- [9] Buch A.: Zagadnienia wytrzymałości zmęczeniowej. PWN, Warszawa 1964.
- [10] Brzoska Z.: Wytrzymałość materiałów. PWN, Warszawa 1972.